Analysis of Circulating Protein Aggregates Reveals Pathological Hallmarks of Amyotrophic Lateral Sclerosis

Rocco Adiutori
Barts and The London School of Medicine and Dentistry Blizard Institute
Fabiola Puentes
Barts and The London School of Medicine and Dentistry Blizard Institute
Michael Bremang
Proteome Sciences plc
Vittoria Lombardi
Barts and The London School of Medicine and Dentistry Blizard Institute
Irene Zubiri
Barts and The London School of Medicine and Dentistry Blizard Institute
Emanuela Leoni
Proteome Sciences R&D GmbH & Co. KG
Johan Aarum
Karolinska institutet Department of Clinical Microbiology
Denise Sheer
Barts and The London School of Medicine and Dentistry Blizard Institute
Simon McArthur
Barts and The London School of Medicine and Dentistry Blizard Institute
Ian Pike
Proteome Sciences plc
Andrea Malaspina (a.malaspina@qmul.ac.uk)
Queen Mary University of London https://orcid.org/0000-0002-8020-7567

Research article

Keywords: Biomarkers, neurodegeneration, protein aggregates, amyotrophic lateral sclerosis, MS-based proteomics, TMT Calibrator proteomics

Posted Date: September 18th, 2020

DOI: https://doi.org/10.21203/rs.3.rs-71596/v1

Abstract

Background: plasma proteins composition reflects the inflammatory and metabolic state of an organism and can be predictive of system-level and organ-specific pathologies. Circulating protein aggregates (CPA) are enriched with heavy chain neurofilaments (NfH), axonal proteins involved in brain protein aggregates (BPA) formation and recently identified as biomarkers of the fatal neuromuscular disorder amyotrophic lateral sclerosis (ALS).

Methods: here we use mass spectrometry and brain-enhanced TMTcalibrator™-based proteomics to evaluate the composition and the brain-derived protein component of CPA extracted from ALS and healthy controls (HC) plasma samples using high-performance ultracentrifugation. We also test CPA and BPA proteins aggregation propensity and the resistance to proteases digestion by trypsin, chymotrypsin, calpain and enterokinase of NFH within aggregates. Finally, we study CPA biological effects on neuronal and endothelial cell lines.

Results: electron microscopy confirms the presence in CPA of electron-dense macromolecular particles appearing as either large globular or as small filamentous formations. CPA from ALS are enriched with proteasome system proteins while HC CPA show a prominent expression of proteins involved in metabolism. CPA enterokinase digestion in ALS generates 171 and 31 KDa NfH fragments not seen in HC samples. Compared to the whole human proteome, proteins within CPA and BPA show distinct chemical features of aggregation propensity, which appear dependent on the tissue or fluid of origin and not on the healthy or pathological source of plasma. The use of a TMTcalibrator™ proteomics workflow reveals 4973 brain-derived low-abundance proteins in CPA, including products of translation of 24 ALS risk genes. 285 (5.7%) are regulated in ALS ($p < 0.05$) and belong to biochemical pathways previously linked to ALS pathogenesis and aggregates formation. CPA from both ALS and HC have a higher effect on hCMEC/D3 endothelial and PC12 neuronal cells viability than immunoglobulins extracted from the same plasma samples. Compared to HC, CPA from ALS plasma samples exert a higher toxic effect on both cell lines at lower concentrations.

Conclusions: this study demonstrates that CPA are significantly enriched with brain proteins which are representative of ALS pathology and a potential source of biomarkers and therapeutic targets for this incurable disorder.

Background

Stratification of clinically heterogeneous neurodegenerative disorders into more homogeneous and predictable disease phenotypes is an essential pre-requisite for clinical trials (Bradley, 2012). As disease progression in Amyotrophic Lateral Sclerosis (ALS), a fatal neurodegenerative disorder, and in Alzheimer's disease may be linked to the spread of pathological protein aggregation in brain, the detection in biofluids of aggregate-bound proteins like neurofilaments (Nf), tau and beta amyloid, has proved a successful strategy for biomarkers discovery (Lee & Kim, 2015; Polymenidou & Cleveland, 2011). (Friedrich et al.,

2010). Brain proteins like neurofilaments (Nf) can leak from pathological aggregates within neurons and axons into cerebrospinal fluid (CSF) and blood. In biofluids, proteins including Nf may assemble into circulating protein aggregates (CPA), similarly to what described for stress granule-like formations (Yang & Hu, 2016). Using ultracentrifugation (UC) and low-complexity binders to extract CPA from plasma of healthy individuals, we have recently shown that CPA are enriched with heavy chain neurofilament (NfH) and not with the light and medium isoforms (NfL, NfM) (Adiutori et al., 2018). We have also demonstrated that the change in biofluid levels of Nf in relation to the speed of disease progression can be used for the clinical stratification of ALS (C. H. Lu, Macdonald-Wallis, et al., 2015; C. H. Lu, Petzold, et al., 2015).

Both brain tissue and biological fluids have been reported to show an age-dependent increase in protein aggregation (Xia, Trasatti, Wymer, & Colon, 2016). The loss of solubility of proteins may relate to the reduction in chaperonal and homeostatic functions of specific proteins, like for example albumin, which is abundant in plasma (Finn, Nunez, Sunde, & Easterbrook-Smith, 2012). The increase of aggregation propensity of proteins with age is key to understand the pathobiology of neurodegeneration. In ALS, protein aggregation is an important pathological feature and age is probably the main risk factor to develop the disease (Niccoli, Partridge, & Isaacs, 2017; Xia et al., 2016). Age-associated changes in plasma protein composition have recently been investigated in a large cohort of individuals of a wide age range, leading to the identification of clusters of proteins whose expression is associated with an individual's biological age and with the health status of different organs including the brain (Lehallier et al., 2019; Williams et al., 2019).

Unlike whole plasma, the proteome of biological fluids aggregates has not been well documented. Our recent proteomic analysis of CPA from neurologically healthy individuals has identified proteins involved in biological processes described in most neurodegenerative disorders, including cell structural and extra-cellular matrix proteins with prion-like behavior, or involved in inflammatory responses and in the phagosome pathway (A. McCombe & D. Henderson, 2011; Adiutori et al., 2018; Amor et al., 2014; Lyon, Wosiski-Kuhn, Gillespie, Caress, & Milligan, 2019). Based on the data reported above, we could speculate that plasma is a carrier of biologically active proteins, which are informative of the physiological and pathological state of organs. Indeed, previous studies have shown that proteins in circulation can influence the regenerative capacity of multiple tissues and organs in mice (Conboy et al., 2005; Villeda et al., 2011). Biologically active plasma proteins may also cause or facilitate the reported increase in blood brain barrier (BBB) permeability observed with ageing and in ALS (Garbuzova-Davis et al., 2012).

Here we test the hypothesis that those proteins compartmentalized within aggregate-like particles in blood may provide clues on the pathobiology of a neurodegenerative disorder like ALS and a new source of disease biomarkers, as already shown for brain protein aggregates. We show that CPA contain up to 5,000 brain-derived proteins, a proportion of which are regulated in ALS and/or linked to ALS-risk genes. We also describe an ALS-specific pattern of NfH enterokinase proteolysis in CPA and the biological effect that these formations have in brain and endothelial cell cultures.

Materials And Methods

Patients and biological samples

Samples were collected from individuals with a diagnosis of amyotrophic lateral sclerosis (ALS) according to established criteria (Ludolph et al., 2015) and from healthy controls (HC), enrolled in the ALS biomarkers study (REC n. 09/H0703/27). Participants had no known neurological comorbidities, nor were they affected by systemic or organ-specific autoimmune disorders (Supplementary Table 1–3). Blood was drawn by venipuncture in EDTA tubes, processed within 2 hours by spinning at 3500 rpm for 10 minutes at 20 °C and stored at -80 °C. Pre-central Gyrus brain tissue samples from two individuals affected by ALS (Brain1 and Brain2) obtained from The Netherlands Brain Bank (Netherlands Institute for Neuroscience, Amsterdam - www.brainbank.nl) were included in the study.

Enrichment of protein aggregates

As previously reported, circulating protein aggregates (CPA) were enriched from plasma using a high concentration of detergent (Triton X-100) to dissolve vesicles and protein complexes and ultracentrifugation (UC), to exploit the density of the detergent-resistant particles (Adiutori et al., 2018) (details in the Supplementary Material). The same protocol was applied to brain samples after mechanical homogenisation in 0.8 M NaCl, 1% Triton X-100, 0.1 M Ethylenediaminetetraacetic acid (EDTA), 0.01 M Tris at pH 7.4 and proteinase inhibitor (cOmplete™, Merck).

Quantification of CPA protein content

The protein aggregate fractions resuspended in 8M urea were tested using Pierce™ BCA Protein Assay Kit (ThermoFisher) for total protein quantitation.

Transmission Electron Microscopy (TEM)

A glow-discharged 400 mesh grid coated with carbon was incubated with a droplet of aggregates-enriched sample and after 10 seconds, the excess was removed by carefully touching to the grid edge with filter paper. Negative staining was obtained incubating the grid with a droplet of 2% w/v uranyl acetate (UA). After washing with ddH2O, the grid was air-dried at room temperature and micrographs acquired by a JEOL JEM 1230 electron microscope.

Circulating and brain protein aggregates protease digestion

Aggregates-enriched fractions were enzymatically digested using trypsin (V542A, Promega), α-Chymotrypsin (referred as Chymotrypsin in the text, C4129, Sigma), Calpain (208712, Millipore) and Enterokinase (11334115001, Roche). To minimize UC-induced protease resistance, for disrupting disulphide bonds and enhance cleavage sites accessibility, pellets were first re-suspended in 50 µl of each protease enzyme recommended buffer (PBS for Trypsin, 100 mM Tris HCl for Chymotrypsin, 50 mM Hepes – 30 mM NaCl for Calpain and 50 mM Tris HCl for Enterokinase) and 5 µl of 0.5 M DTT was then added prior to sonication. Finally, each enzyme was added into the digestion reaction mix tube at a ratio

1:20 protease:total protein. 5.5 µl of 0.1 M CaCl2 were added to the chymotrypsin and calpain reaction mixes for enzyme activation as indicated by the manufacturers. Digestion mixes were subsequently incubated overnight at 37 °C and later stopped adding loading buffer 4X (Fisher Scientific), dithiothreitol (DTT) and by heating at 95 °C for 10 minutes. Resistance to proteases of NfH CPA content was tested by western blotting and results adjusted to protein and NfH content (Supplementary Material).

Western blotting

Proteins loaded onto gels were transferred after electrophoresis to a polyvinylidene difluoride (PVDF) membrane and then blocked with 5% skimmed milk in Tris-Buffered Saline (TBS) 0.1% Tween-20 buffer (TBS-T 0.1%) at room temperature for 1 hour. Incubation was performed overnight with primary antibody at 4 °C and with secondary antibody for 1 hour at RT. Membranes were washed with TBS-T 0.1% and incubated with enhanced chemiluminescence substrate. Imaging was undertaken using Image Lab (Bio-Rad) and bands volume measured using the “Volume Tools” function in Image Lab and “Adj. Vol. (Int)”. Antibodies used in this study are listed in Supplementary Table 6.

MS-based proteomics

To evaluate protein composition of the enriched protein aggregate fractions from plasma and brain, we have first undertaken LC-MS/MS analysis after in-gel trypsin digestion of pooled plasma samples (PPS) CPA from ALS and HC individuals as well as of brain protein aggregates (BPA). We have then applied TMTcalibrator™ proteomics on individual ALS and HC CPA samples using ALS brain lysate as ion source (calibrant).

In-gel trypsin digestion

Samples were loaded onto a gel for electrophoresis and gel bands were cut out. Subsequently, disulfide bonds reduction with DTT and alkylation with Iodoacetamide (IAA) was performed. After washing and complete de-staining, each gel piece was rehydrated with a 50 mM ammoniumbicarbonate (Ambic) solution and treated with 0.01 µg/µl Trypsin (V542A, Promega) during overnight (ON) incubation at 37 °C. Tryptic peptides were recovered and each sample was freeze-dried in a vacuum centrifuge for LC-MS/MS analysis.

TMTcalibrator™

TMTcalibrator™ workflow was developed by Proteome Sciences plc (Leoni et al., 2019; Russell et al., 2016; Zubiri et al., 2018) to quantify low-abundance peptides in matrices with a high degree of biological complexity. Two ten-plexes were set up, each containing 1) lysate of two ALS brain tissue samples mixed 1:1 loaded at high concentration in 4 channels (calibrant samples) and 2) CPA from ALS patients and HC individuals (analytical samples; Supplementary Fig. 1). The calibrant samples were prepared by dissolving brain tissues in SysQuant Buffer, removing the debris and mixing the two samples 1:1 (w/v): (w/v), while CPA were obtained as described above. SysQuant Buffer was used to dilute 40 µg of total protein for each analytical sample and 840 µg for the brain calibrant in each of the two ten-plexes. After

reduction with DTT and alkylation with IAA, desalting with SepPak tC18 was carried out and the calibrant divided into four different aliquots with a 1:4:6:10 volume ratio.

Dried samples were re-solubilised in 120 µl KH_2PO_4 and TMT reagents were added combining a specific tag for each sample (Supplementary Fig. 1) and reactions were stopped adding hydroxylamine to a final concentration of 0.25% (w/v). At this stage the samples included in each ten-plex were merged and were fractionated by basic Reverse Phase (bRP) using Pierce™ High pH Reversed-Phase Peptide Fractionation Kit (ThermoFisher Scientific), generating eight fractions for each of the two ten-plexes.

LC-MS/MS analysis was performed in double-shot using a Thermo Scientific™ Orbitrap Fusion Tribrid (Thermo Scientific) mass spectrometer coupled to an EASY-nLC 1000 (Thermo Scientific) system. The 16 bRP fractions were resuspended in 2% ACN, 0.1% formic acid (FA), and then 12 µg from each was injected into a 75 µm × 2 cm nanoViper C18 Acclaim PepMap100 precolumn (3 µm particle size, 100 Å pore size; P/N 164705; Thermo Scientific). Peptides were separated at a flow rate of 250 ml/min and eluted from the column over a 5 hours gradient starting with 0.1% FA in ACN (5–30% ACN from 0 to 280 min followed by 10 min ramping up to 80% ACN) through a 75 µm × 50 cm PepMap RSLC analytical column at 40 °C (2 µm particle size, 100 Å pore size; P/N ES803; Thermo). After electrospray ionisation, MS spectra ranging from 350 to 1500 m/z values were acquired in the Orbitrap at 120 k resolution and the most intense ions with a minimal required signal of 10,000 were subjected to MS/MS by HCD fragmentation in the Orbitrap at 30 k resolution. Protein identification was carried out with Thermo Scientific Proteome Discoverer 1.4.

Bioinformatics

LC-MS/MS analysis generated 32 files that were processed by Proteome Sciences' proprietary workflows for TMTcalibrator™ including the Calibrator Data Integration Tool (CalDIT), Feature Selection Tool (FeaST) and Functional Analysis Tool (FAT) (Leoni et al., 2019; Zubiri et al., 2018) (Supplementary Fig. 2). All raw spectra were searched against the human FASTA UniProtKB/Swiss-Prot using SEQUEST-HT and raw intensity values were measured through the TMT reporter ions.

Aggregation propensity

To study the chemical properties of the protein mix within the CPA which affect their propensity to aggregate, in-silico analysis of protein size, isoelectric point (pI) and hydrophobicity was undertaken using Uniprot – ExPASy (Compute pI/MW web tool and GRAVY score - http://www.gravy-calculator.de). This analysis was undertaken comparing the ALS, HC CPA and BPA protein lists to the entire Uniprot human proteome (reviewed sequences only).

IgG extraction from plasma and quantification

IgG extraction from the plasma samples CPA were extracted from was undertaken using Protein G Spin Columns (Thermo Scientific, UK) following the manufacturer's protocol. The fraction of purified antibodies was quantified measuring the relative absorbance of each fraction at 280 nm and the buffer

exchanged into PBS using Amicon Ultra centrifugal filter with 100 KDa molecular weight cut-off (Millipore Merck, UK).

PC12 viability

Undifferentiated PC12 cells were cultured in Dulbecco's modified Eagle's medium (Invitrogen, Paisley, UK) supplemented with 10% fetal calf serum (Invitrogen) and 10% horse serum (Sigma), 100 µg/ml streptomycin, 100 U/ml penicillin (Invitrogen) and incubated at 37° in a 5% CO_2-humidified atmosphere. Differentiation was obtained by plating at a density of 3×10^5 cells/well in 96-well plates (Nunc, Thermofisher, UK) in Dulbecco's modified Eagle's medium (0,1% horse serum supplemented with nerve growth factor, 50 ng/ml). Cells were treated for 24 hours at RT with CPA dissolved in Urea 8M or with IgG in medium. Viability was tested incubating with 0.5 mg/ml 3-(4,5-dimethylthiazol-2-yl)-2,5 diphenyltetrazolium bromide (MTT) for 4 h. Supernatants were discarded and 200 µl DMSO added to solubilize formazan crystals. Colorimetric changes were measured at 590 nm (Synergy HT microplate reader). The percentage of cell viability was calculated as the absorbance of treated cells/absorbance of control.

Endothelial cell viability

Human cerebromicrovascular endothelial cell lines hCMEC/D3 were maintained and treated as described previously (Hoyles et al., 2018; Weksler et al., 2005). Cells were plated on plastic coated with 0.06 µg/cm^2 calf skin collagen type I (Sigma, UK) and were cultured to confluency in complete endothelial cell growth medium MV2 (PromoCell GmbH, Germany). Following treatment for 24 h with aggregates or IgG in medium, cell number was estimated using the Prestoblue HS Cell Viability assay (ThermoFisher Scientific Ltd., UK) according to the manufacturer's instructions and using a CLARIOstar fluorescence microplate reader (BMG Labtech Ltd., UK) with excitation and emission filters set to 560 nm and 590 nm respectively.

Statistics

The enriched KEGG pathways obtained from the submission of ALS and HC pools protein lists to Webgestalt were evaluated for statistical significance using the hypergeometric test (Zhang, Kirov, & Snoddy, 2005). To test differences in aggregation propensity across proteomes, data were analysed for normality using the Shapiro-Wilk test. Non-parametric group analysis was performed using Kruskal–Wallis one-way test of variance and Dunn's multiple comparison as post-test (GraphPad-v7). To test ALS versus HC proteolytic bands intensity difference, a "t-Test - Two-Sample Assuming Unequal Variances" was performed. Principal component analysis (PCA) was used to study the variance of the data sets generated by the TMTcalibrator™ workflow. To determine the regulated features by FeaST, LIMMA considered the following linear model: logRatio(ALS/HC) ≈ class + group + gender + progression rate + TMT batch. Multiple testing corrections and false discovery rate (FDR) were obtained using the Benjamini-Hochberg procedure. For the Functional analysis (FAT), a two-sided p-value was generated by the Mann Whitney U test and the Benjamini-Hochberg method was used for multiple test correction. Expression values were normalised with other 1000 randomly selected background expression values. A minimum of three matched identifiers (e.g. gene names) were required for each term. Terms with an

adjusted p-value < 0.3 were considered significant. Cell survival assays were evaluated by two-way ANOVA and Tukey HSD test.

Availability of data and materials'

The datasets supporting the conclusions of this article are available in the PRIDE repository, PXD018938 and PXD018923.

Study approval

A written informed consent was obtained from all ALS and HC participants enrolled in the ALS biomarkers study (REC n. 09/H0703/27). Written informed consent was obtained from donors of brain samples for the use of the material and clinical information for research purposes (Netherland Brain Bank: 2009/148).

Results

Study participants

The mass spectrometry (MS)-based proteomic study of CPA was performed on 2 pools of plasma samples (PPS), one containing samples from three fast and three slow progressing ALS individuals and one from six HC individuals (ALS: 5 males (M), 1 female (F); HC: 3M, 3F; age range: ALS: 46.1–78.5; HC 51.8–62.9; Supplementary Table 1).

For the TMT® proteomic experiment, for protease digestion and for validation by western blot, CPA extracted from plasma samples from ALS and HC cohorts (male/female ratio: 3:3; age range: ALS 60.2–68.8; HC: 60.6–68.3; Supplementary Tables 2 and 3) were tested individually.

Extraction of circulating (CPA) and brain protein aggregates (BPA): qualitative analysis by transmission electron microscopy

To verify the efficiency of CPA and BPA extraction protocols, we have used transmission electron microscopy (TEM) to visualize the aggregate fractions after UC of plasma samples (3 HC and 3 ALS cases) and ALS brains. TEM revealed the presence of (macromolecular) amorphous electron-dense particles of different size, in both CPA and BPA (Fig. 1A and B respectively). With the same extraction protocol, in CPA but not in BPA grids, it was possible to appreciate small, round (few nm diameter) particles close or superimposed to the bigger, globular and more electron-dense bodies. As previously reported, these formations may represent micelles composed of lipids, detergents or lipoproteins (Safar et al., 2006; Terry et al., 2016) (Fig. 1A and B), such as very low-density (VLDL), low-density (LDL) and high-density lipoproteins (HDL). Both lipoproteins and biochemical pathways linked to their metabolism were in fact detected and found significantly regulated in the CPA proteomic study (described below). Unlike the large, amorphous, globular appearance of CPA aggregates, some of the electron-dense formations in

the BPA micrographs had filamentous and donut-like shapes (Fig. 1B and C), suggestive of contamination with ferritin of brain homogenates as previously reported (Quintana, Cowley, & Marhic, 2004; Sana, Poh, & Lim, 2012; Zhou et al., 2009). In CPA grids only, it was possible to see filamentous fragments with a rough surface similar to those seen in BPA (Fig. 1D, E and F).

Circulating protein aggregates (CPA) and brain protein aggregates (BPA) composition: LC-MS/MS proteomics

Liquid Chromatography coupled with Tandem Mass Spectrometry (LC-MS/MS) after in-gel trypsin digestion was used to study protein aggregates enriched from ALS and HC pooled plasma samples (PPS) as well as from ALS brains. In total, 367 proteins were identified in ALS CPA and 353 in HC CPA (Fig. 2A). 264 (57.9% of the total) proteins were expressed in both ALS and HC CPA (here defined as shared), while 103 (22.6%) were found only in ALS (defined as unique ALS) and 89 (19.5%) in HC CPA (defined as unique Controls) (Fig. 2A). Functional analysis of these protein sub-sets was performed using Webgestalt for Kyoto Encyclopaedia of Genes and Genomes (KEGG) pathway enrichment. Among the most enriched pathways, the proteasome was the most significantly represented feature in ALS ($p = 0.028$; four genes matched in this category) while the glycolysis/gluconeogenesis pathway ($p = 0.009$; seven genes matched), the pentose phosphate pathway ($p = 0.003$; five genes matched) and the carbon metabolism ($p = 0.008$; eight genes matched) were significantly expressed in HC. Proteins previously linked to ALS like NfH or TDP-43 were not detected.

LC-MS/MS identified 48 protein groups in brain protein aggregates (BPA), including the three neurofilament isoform proteins. There was little overlap between CPA and BPA proteins (Fig. 2B), with only five proteins identified in both types of aggregates, one identified in both ALS CPA and BPA and one in both HC CPA and BPA.

Aggregation propensity

The brain and plasma aggregate protein lists generated by LC-MS/MS were studied to test the propensity to aggregation in each dataset. The distribution of protein size or molecular weight (MW), isoelectric point (pI) and hydrophobicity, expressed as GRAVY index, were analysed in each proteome dataset with the whole human proteome as reference (Weids, Ibstedt, Tamas, & Grant, 2016). BPA had a significantly higher MW ($p < 0.0001$) compared to the other datasets (ALS, HC, shared respectively and Human proteome, Fig. 3A), while pI was significantly lower in all CPA datasets compared to the Human proteome ($p < 0.0001$; Fig. 3B). Despite minimal overlap in protein composition between CPA and BPA (Fig. 2B), aggregation propensity in the two aggregate types and in the human proteome was similar when measured by GRAVY index, which takes into account the average hydropathy of a peptide according to its aminoacidic composition (Fig. 3C).

CPA protease digestion and NfH resistance

Resistance to protease digestion has been described as a key feature of altered protein behavior in conditions like prion disease (McKinley, Bolton, & Prusiner, 1983). We have previously shown that neurofilament heavy chain (NfH) is found in blood CPA (Adiutori et al., 2018; C. H. Lu, Kalmar, Malaspina, Greensmith, & Petzold, 2011). As NfH is constitutively expressed in protein aggregates from ALS brain and has been linked to the pathogenesis of the disease, we looked at NfH protease resistance in CPA from ALS and compared its digestion profile to that in HC CPA (Fig. 4). CPA enriched from the ALS and HC plasma samples were treated with trypsin, chymotrypsin, enterokinase and calpain. Both CPA NfH digested and undigested profiles were analysed.

Western blot analysis of NfH in plasma CPA before digestion detected three bands at 460, 268 and 41 KDa as previously reported (Fig. 4A) (Adiutori et al., 2018). The sum of all NfH band intensities (SUM) was (not significantly) higher in the ALS group compared to HC. The ratio between the intensity of the 460 KDa band and the NfH SUM intensity (460/SUM) was higher in HC, while the ratio between the intensities of the 268 and 460 bands (268/460) was significant higher in ALS (Fig. 4A).

Treatment with trypsin or chymotrypsin showed an almost complete digestion of NfH in both ALS and HC, with the exception of a residual 41 KDa band present in a minority of samples (data not shown). After calpain digestion, there was a different pattern of immunoreactivity for each CPA sample with the exception of 58 and 41 KDa bands evenly detected in all samples (Fig. 4B). Enterokinase digestion resulted in a 49 KDa band in all samples with equal expression in ALS and HC (Fig. 4C). All ALS samples showed bands at 171 and 31 KDa not seen in HC samples (Fig. 4C).

NfH in BPA showed low or no resistance to digestion with all three enzymes (Fig. 4D). Chymotrypsin and enterokinase digestions (Fig. 4D, lane 2 and 3 respectively) generated no distinct bands but a faint smear at higher molecular weight than the NfH bands detected in undigested brain and brain lysate (Fig. 4D, lane 1 and 5 respectively). Calpain digestion showed two faint bands at about 171 KDa (Fig. 4B, lane 4).

TMTcalibrator™: brain-derived proteins in CPA

The observed lack of similarity in the composition of brain and plasma aggregates may relate to the limits of proteomic techniques, whereby low abundance (brain-derived) proteins, may be masked by those with high abundance and detection confounded by the presence of post-translational modifications. To address these shortfalls and gather more information on the potential enrichment of brain-derived proteins in circulating aggregates, we have undertaken further proteomics using a TMTcalibrator™ workflow, where brain lysate was used to enhance detection of proteins in CPA (Leoni et al., 2019; Russell et al., 2016; Zubiri et al., 2018).

4973 brain-derived proteins were identified, including the three neurofilaments (Nf) protein isoforms (Nf Light (NfL), Nf Medium (NfM) and Nf Heavy (NfH). Nf were found at a relatively higher level in ALS compare to HC samples (log2-fold change ALS/HC (logFC) = 0.093, 0.181 and 0.298, respectively) but none was significantly regulated ($p = 0.40$, 0.16 and 0.06 respectively). Of the 4973 brain-derived proteins, 285 proteins (5.7%) showed a statistically significant regulation ($p < 0.05$). 158 were more expressed in

HC (logFC < 0) with an average fold-change (FC) of -0.667, while 127 in ALS (logFC > 0) with an average FC of 0.703. The protein list obtained was matched with an ALS gene list obtained from the MalaCards database, an integrated repository of human diseases and their annotations. 24 ALS proteins were identified including Fused in Sarcoma RNA-binding protein (FUS), which was found to be significantly upregulated in ALS ($p = 0.00696$) (Table 1).

Table 1
ALS risk genes included in the list of proteins identified by the TMTcalibrator™ workflow

[A]Gene	[B]Uniprot ID	[C]Protein name	[D]Unique peptides	[E]logFC	[F]p-value
FUS	P35637-2	Isoform Short of RNA-binding protein FUS	5	0.564	6.96e-03
NEFH	P12036	Neurofilament heavy polypeptide	27	0.298	6.36e-02
OPTN	Q96CV9	Optineurin	11	-0.243	9.58e-02
UNC13A	Q9UPW8	Protein unc-13 homolog A	11	-0.326	9.75e-02
PON2	Q15165-3	Isoform 3 of Serum paraoxonase/arylesterase 2	1	0.292	1.46e-01
ANG	P03950	Angiogenin	1	-0.595	1.67e-01
CHMP2B	Q9UQN3	Charged multivesicular body protein 2b	1	0.492	1.90e-01
VCP	P55072	Transitional endoplasmic reticulum ATPase	65	-0.514	2.16e-01
ATXN2	Q99700-2	Isoform 2 of Ataxin-2	2	-0.445	2.51e-01
ANXA11	P50995-2	Isoform 2 of Annexin A11	16	0.150	3.01e-01
SOD1	P00441	Superoxide dismutase [Cu-Zn]	8	0.176	3.39e-01
ERBB4	Q15303-4	Isoform JM-B CYT-2 of Receptor tyrosine-protein kinase erbB-4	1	-0.284	3.70e-01
TARDBP	Q13148	TAR DNA-binding protein 43	2	0.180	3.85e-01
SQSTM1	Q13501	Sequestosome-1	2	-0.280	4.00e-01

[A]Gene	[B]Uniprot ID	[C]Protein name	[D]Unique peptides	[E]logFC	[F]p-value
MATR3	P43243	Matrin-3	16	0.127	4.03e-01
PFN1	P07737	Profilin-1	14	0.136	4.08e-01
VAPB	O95292	Vesicle-associated membrane protein-associated protein B/C	10	-0.094	4.31e-01
EPHA4	P54764	Ephrin type-A receptor 4	13	-0.082	5.37e-01
PON1	P27169	Serum paraoxonase/arylesterase 1	14	0.123	6.07e-01
TAF15	Q92804-2	Isoform Short of TATA-binding protein-associated factor 2N	3	0.067	6.99e-01
UBQLN2	Q9UHD9	Ubiquilin-2	4	-0.065	6.99e-01
HNRNPA1	P09651-3	Isoform 2 of Heterogeneous nuclear ribonucleoprotein A1	8	-0.066	7.50e-01
DCTN1	Q14203-6	Isoform 6 of Dynactin subunit 1	2	0.020	9.34e-01
TBK1	Q9UHD2	Serine/threonine-protein kinase TBK1	5	-0.004	9.86e-01

ALS risk genes included in the list of proteins identified by the TMTcalibrator™ workflow in CPA from ALS and HC and reported in the gene classifiers MalaCards Human Disease Database (https://www.malacards.org/card/amyotrophic_lateral_sclerosis_1#RelatedGenes-table) (Database, n.d.). Among a total of 38 ALS elite genes reported in the MalaCards Human Disease Database (those more likely to cause the disease), 24 were detected in the list of proteins generated by the TMTcalibrator™ experiment.

A: the gene symbol used to represent a gene

B: Uniprot database protein identifier

C: protein full name recommended by Uniprot

D: number of peptide sequences unique to a protein group

E: relative quantification with value expressed as log2(ALS/HC) intensities

F: statistical significance for differential regulation between ALS and HC experimental groups

Principal component analysis (PCA) of the proteomic data after correction for the TMT® batch-effect identified the sample origin (ALS or HC) as the strongest component (41.17%) of the total variance in the data matrix (Fig. 5A). The marked separation between ALS and HC in CPA brain-derived proteins identified by PCA was also observed when using clustering of these regulated proteins (Fig. 5B). Considering the CPA enrichment of brain proteins (Fig. 5C), we speculate that circulating protein assemblies represent a good source of biomarkers for ALS, which may be difficult to detect in whole plasma analysis.

Table 1. **ALS risk genes included in the list of proteins identified using the TMTcalibrator™ workflow**

Functional analysis

We have assessed the relevance of different biological terms in the proteomic data, based on their over-representation in the subset of regulated proteins (Leoni et al., 2019; Zubiri et al., 2018). Within the top ten regulated biochemical pathways of the 69 identified ($p < 0.05$), five were involved in metabolism of lipoproteins (Supplementary Table 7). Several authors already described that metabolism in ALS is switched from sugars and carbohydrates to lipids use (Delaye et al., 2017; Szelechowski et al., 2018; Tefera & Borges, 2017). Within the 69 pathways highlighted by FAT, we have looked at highly regulated protein (unique peptides ≥ 2, LogFC < -0.693 or > 0.693, p-value < 0.05) to evaluate other pathways potentially involved with aggregation and neurodegeneration, but also to obtain potential targets for patient stratification. We identified 48 proteins (Supplementary Table 8) from which we could highlight four biochemical pathways: metabolism of carbohydrates ($p = 0.0099$), glycosaminoglycans (GAGs) metabolism, lysosome ($p = 0.0015$), synthesis of phosphatidic acid (PA; $p = 0.0184$) and wnt signalling pathway ($p = 0.0337$). GAGs are involved in protein aggregation and prion diffusion (Ancsin, 2003; DeWitt, Richey, Praprotnik, Silver, & Perry, 1994; Forostyak et al., 2014; Foyez et al., 2015; Hirano et al., 2013; Holmes et al., 2013; Nishitsuji, 2018; Sarrazin, Lamanna, & Esko, 2011; Shijo et al., 2018). Lysosome activity changes have been described in ALS caused by the C9orf72 gene repeat expansions (Cipolat Mis, Brajkovic, Frattini, Di Fonzo, & Corti, 2016; Sasaki, 2011; Shi et al., 2018; Song, Guo, Liu, & Tang, 2012; Sullivan et al., 2016), while synthesis of PA and related phospholipids, including phosphatidylcholine and phosphatidylethanolamine, have been linked to ALS and prion disease pathogenesis (Blasco et al., 2017; Supattapone, 2012).

Proteomic results validation by immunoassays

Six proteins belonging to ALS-relevant molecular pathways were tested by western blot: Glypican-4 (GPC4), Fibromodulin (FMOD), Biglycan (BGN), Cation-dependent mannose-6-phosphate receptor (M6PR), Endophilin-B2 (SH3GLB2) and Protein DJ-1 (PARK7) using CPA extracted from ALS patients and HC, with brain lysate as reference. SH3GLB2 showed the same trend of ALS vs HC protein regulation identified in the TMTcalibrator™ experiment, with a similar level of regulation (logFC = 0.34 in TMTcalibrator™ and log2(ALS/HC) = 0.437) in western blot analysis (Fig. 6). The remaining proteins showed a different trend of regulation compared to that obtained in the proteomic analysis (data not shown). SH3GLB2 and M6PR

were detected at a higher MW in CPA compared to brain lysate, possibly in keeping with a different PTM profile in tissues as opposed to fluids which may affect the state of aggregation and protease digestion.

Aggregation propensity of the brain-derived proteins in CPAs

We evaluated aggregation propensity of the CPA proteins identified by TMTcalibrator™ compared to the Human proteome and BPA, using the reported physicochemical parameters. The analysis was performed on the entire TMT® proteome dataset and on the 285 regulated proteins only, which were divided in two groups based on the level of differential expression: log(ALS/HC) > 0 and log(ALS/HC) < 0. There was no statistically significant difference among these three datasets for the parameters under investigation. However, the entire TMT and BPA proteome datasets showed statistically significant higher MW and lower pI compared to the Human proteome ($P < 0.0001$), while for GRAVY index, the BPA values were lower than TMT and Human proteome ($p = 0.0348$ and 0.0224, respectively; data not shown).

Cell survival assays

To test the biological effects of CPA on living cells, human brain microvascular endothelial cells (hCMEC/D3) modelling human blood-brain barrier (BBB) and PC12 neuron-like cells lines were treated with CPA from ALS patients and HC and cell viability measured (Fig. 7). Total IgG were extracted from the same blood samples CPA were separated from and used to treat the same cell lines. CPA re-suspended in PBS were administered at defined concentrations to hCMEC/D3, while CPA were pre-treated with 8M urea before testing PC12 viability. Dissolution of aggregates by urea for PC12 cells was undertaken to evaluate the effect of CPA-containing proteins rather than the effect of their aggregated state. PC12 cell viability decreased at increasing concentration of CPA, (to 75% at 0.5 µg/ml; Fig. 7B), while endothelial cells showed the opposite trend, with the maximum effect on cell viability at the lowest concentration (0.05 µg/ml) and no effect at the highest concentration (1 µg/ml; Fig. 7A). ALS CPA exerted higher toxicity (lower cell viability) at lower concentration (0.05 µg/ml) with endothelial cells and with PC12 cells (0.5 µg/ml) compared to HC CPA (Fig. 7). IgG extracted from the same ALS and HC plasma samples as CPA, showed reduction of endothelial cell viability to 80% and to between 70 and 85% in PC12 cells at 1.5 µg/ml, with no significant difference between ALS and HC (Fig. 7).

Discussion

In this paper we show that in ALS, an incurable neurodegenerative disorder, circulating protein aggregates (CPA) are enriched with proteins implicated in the proteasome system, an essential clearance mechanism of defective proteins (Ling, Polymenidou, & Cleveland, 2013; Saez & Vilchez, 2014). Using a TMTcalibrator™ proteomic approach we also show, for the first time, that these aggregates contain just below 5,000 brain peptides, including a significant number of proteins linked to ALS risk genes such as FUS and SOD1 (Table 1). Chemical features defining propensity to aggregate of CPA proteins differ from those seen in brain aggregates and from the whole human proteome. Plasma CPA and particularly low

concentration ALS CPA, affect both endothelial and neuronal cells viability, showing a more pronounced biological effect than that observed using the immunoglobulin fraction extracted from the same plasma samples (Fig. 7).

The TMTcalibrator™ workflow employed in this study has the added value of being able to analyze tissues and fluids in the same experiment, enhancing the detection of low-abundance fluid proteins that are also expressed in brain, most of them undetectable using standard proteomics (Adiutori et al., 2018). Of these brain proteins, 285 show a significant level of regulation ($p < 0.05$) in ALS compared to controls (Fig. 5). The detection by proteomics of these low-abundance brain proteins in CPA has important methodological implications. For the identification of the same protein targets, immunoassays may suffer from competition of naturally occurring autoantibodies causing epitope sequestration in aggregates and immunocomplexes as recently shown for neurofilaments (C. H. Lu et al., 2011; C. H. Lu, Petzold, et al., 2015). Unlike TMTcalibrator™ enhanced detection based on an internal tissue calibrant, standard MS-based proteomics would, in turn, lack the sensitivity to discriminate low concentration against more abundant proteins. The mismatch between MS and antibody-based peptide recognition is clearly shown in our validation experiment by western blot, where the use of an orthogonal technique of immunodetection does not always confirm the findings on proteomics. This is not surprising considering that these methods may target different peptides of the same protein producing results that may not be congruent. Despite the inherent limitations of our approach, this study provides a novel strategy for biomarker discovery and measurement in ALS, based on the analysis of proteins compartmentalized in aggregates.

The method of aggregates separation employed in our study does not allow the analysis by proteomics of the supernatant from processed samples, due to detergent contamination following CPA extraction. To circumvent this problem, we have previously used low complexity binders for aggregate separation in biofluid, only to observe that the resulting aggregate fraction had a substantially different protein composition to the one obtained by ultracentrifugation, the method of choice of the current study (Adiutori et al., 2018). It is therefore not possible to compare the protein profile of the aggregates and fluid components of the same plasma sample. To circumvent this problem, we have recently used two separate proteomic workflows, including brain-enhanced TMT proteomics, to study the immunological response and the plasma/brain proteome in phenotypic variants of ALS (Leoni et al., 2019). In the whole plasma, we have identified only nine ALS elite genes out of the 24 identified in our CPA study (including Profilin-1 and the Isoform 2 of Heterogeneous nuclear ribonucleoprotein A1). We may therefore speculate that aggregates in blood are more enriched with neuron-derived and disease-specific proteins compared to the fluid component of plasma, making them a more desirable target in the search for ALS biomarkers.

When compared to a healthy state, functional analysis of the plasma CPA proteome from ALS individuals reveals pathological hallmarks of ALS, including changes in the proteasome-dependent protein degradation and in energy metabolism pathways (Ling et al., 2013; Ngo & Steyn, 2015; Palamiuc et al., 2015; Saez & Vilchez, 2014). The TMTcalibrator™ dataset contains regulated features also known to be involved in ALS pathology including lysosome as well as lipoprotein and glycosaminoglycan

metabolisms (Ling et al., 2013; Ngo & Steyn, 2015; Palamiuc et al., 2015; Saez & Vilchez, 2014; Sasaki, 2011; Shi et al., 2018; Sullivan et al., 2016; Szelechowski et al., 2018; Tefera & Borges, 2017) (Supplementary Table 7). To our knowledge, changes in proteasome activity in ALS have so far been shown in such detail only in brain, spinal cord and in neuronal cell lines, but not systemically or more specifically in blood (Ling et al., 2013; Saez & Vilchez, 2014).

The analysis of the physicochemical properties that facilitate proteins aggregation in our protein datasets provides further insight into protein behavior in different molecular environments and in relation with a disease state like ALS. When molecular weight and isoelectric point are taken into account, we observe that the tissue or fluid of origin are the main contributors to the differences in the proteome chemical properties observed across the aggregate types and not the presence or absence of ALS (Fig. 3). When the whole human proteome is included in the analyses as reference, it is possible to see how proteins in the aggregated state are distinguishable from the whole set of human proteins, regardless of their tissue or fluid of origin or presence or absence of a pathological state like ALS. With regard to hydrolytic properties, we have identified clear differences after enterokinase digestion between ALS and HC CPA, with the presence of specific NfH digestion fragments at 171 KDa and at 31 KDa only in ALS samples (Fig. 4C). While a trend for NfH proteolytic fragments over-expression in ALS CPA compared to HC is visible in our experimental data, our study is not powered with enough samples to establish this observation along what already previously reported (C.-H. Lu et al., 2012; C. H. Lu, Petzold, et al., 2015). An extension of this preliminary finding using a larger number of samples will be needed to compare our observation to previously reported data on the same neurofilament isoform enterokinase digestion pattern in a different experimental context (Petzold et al., 2011).

We have tested different cell lines using change in cell viability upon treatment with ALS and HC CPA as a readout of the biological effects of circulating aggregates (Fig. 7). Given that immunoglobulins make up a sizeable share of plasma proteins and that plasma has been shown to have a systemic biological effect (Lehallier et al., 2019; Williams et al., 2019), we have treated the same cell lines with immunoglobulins extracted from the blood samples CPA were recovered from. Whilst immunoglobulins seem not to significantly interfere with cell function at different concentration, there is a detectable toxic effect on PC12 neurons and on hCMEC/D3 endothelial cell cultures upon treatment with CPA, and a clear ALS-specific change in cell viability when CPA are administered at relatively low concentrations (Fig. 7). CPA may well be the proteinaceous component in blood that is ultimately responsible for the BBB damage that has been reported in ALS (Garbuzova-Davis et al., 2012). It is not possible to explain how endothelial cell damage comes into play upon exposure to CPA, and whether the ALS-specific effect relates to a particular composition and/or conformation of aggregates which may be concentration-dependent. The use of TEM to confirm the efficiency of aggregates separation confirms the presence of particles of both globular and filamentous appearance, similar to those observed in BPA (Fig. 1). Further investigation by TEM may be needed to evaluate whether the ALS-specific CPA effect on cells relate to a particular conformation, size or composition of aggregates.

Conclusion

To date, there is no evidence in the literature of investigations into non-membrane bound proteinaceous particles in blood stream of ALS patients and their potential use in biomarkers discovery. Our data indicate that circulating protein aggregates represent a new source of biomarkers enriched with brain proteins, including disease-relevant peptides that can become regulated under pathological condition. These aggregates appear biologically active as they affect endothelial and neuronal cell viability when administered to cell cultures. Further investigation on the nature of these particles will be required to confirm and strengthen this initial finding, including a more extensive comparison with brain aggregates and analysis of the biochemical characteristics in a larger subset of individuals, using more effective and user-friendly methods of CPA extraction.

Abbreviations

ACN
Acetonitrile
ALS
amyotrophic lateral sclerosis
Ambic
ammoniumbicarbonate
BBB
blood brain barrier
BPA
brain protein aggregates
bRP
basic Reverse Phase
CalDIT
Calibrator Data Integration Tool
CPA
Circulating protein aggregates
CSF
cerebrospinal fluid
DMSO
Dimethyl sulfoxide
DTT
Dithiothreitol
EDTA
Ethylenediaminetetraacetic acid
FA
formic acid

FAT
Functional Analysis Tool
FDR
false discovery rate
FeaST
Feature Selection Tool
GAGs
glycosaminoglycans
HC
healthy controls
HDL
high-density lipoproteins
IAA
Iodoacetamide
LC-MS/MS
liquid chromatography-tandem mass spectrometry
LDL
low-density lipoproteins
MTT
3-(4,5-dimethylthiazol-2-yl)-2,5 diphenyltetrazolium bromide
MW
molecular weight
Nf
neurofilaments
NfH
heavy chain neurofilaments
NfL
neurofilament light chain
NfM
neurofilament medium chain

Declarations

Ethics approval and consent to participate

Plasma samples used in the study were collected from individuals enrolled in the ALS biomarkers study (REC n. 09/H0703/27), while Pre-central Gyrus brain tissue samples were obtained from The Netherlands Brain Bank (Netherlands Institute for Neuroscience, Amsterdam - www.brainbank.nl).

Consent for publication

All the authors included gave their consent for publication of this study.

Availability of data and material

The mass spectrometry proteomics data have been deposited in the ProteomeXchange Consortium using PRIDE (Perez-Riverol et al., 2019) partner repository with the dataset identifier PXD018938 and PXD018923.

Competing interests

The authors declare that they have no competing interests.

Funding

This project was funded by the Medical Research Council (MRC) with an Industry CASE Studentship, the Motor Neuron Disease Association (MNDA) UK for the ALS Biomarkers study and the EU2020 for MIROCALS.

Authors' contributions

IP and AM conceived the idea of the present study. RA, MB, VL, IZ, EL, JA, DS, IP and AM designed the experimental plan for aggregates extraction, digestion and proteomics analysis, while RA performed the experiments and MB analysed the proteomics data. RA, FB, VL, SM and AM designed the cell work, while FB and SM performed the experiments. All authors discussed the results and contributed to the final manuscript.

Acknowledgments

We would like to thank the patients and their families along with all healthy donors for their contribution. This study is funded by a Medical Research Council (MRC) Industry CASE Studentship (grant number: MR/M015882/1) awarded to Queen Mary University of London, in collaboration with Proteome Sciences. Plasma samples were obtained from the ALS biomarkers study (09/H0703/27). Support for the development of the methodology outlined in this paper has also come from EU2020 funding (H2020 PHC-13-2014): “Efficacy and safety of low-dose IL-2 (ld-IL-2) as a Treg enhancer for anti-neuroinflammatory therapy in newly diagnosed Amyotrophic Lateral Sclerosis (ALS) patients” (MIROCALS)”.

References

McCombe, P., & D. Henderson, R. (2011). The Role of Immune and Inflammatory Mechanisms in ALS. *Current Molecular Medicine*. https://doi.org/10.2174/156652411795243450

Adiutori, R., Aarum, J., Zubiri, I., Bremang, M., Jung, S., Sheer, D., … Malaspina, A. (2018). The proteome of neurofilament-containing protein aggregates in blood. *Biochemistry and Biophysics Reports*, *14*, 168–

177. https://doi.org/10.1016/j.bbrep.2018.04.010

Amor, S., Peferoen, L. A. N., Vogel, D. Y. S., Breur, M., van der Valk, P., Baker, D., & Van Noort, J. M. (2014). Inflammation in neurodegenerative diseases - an update. *Immunology*. https://doi.org/10.1111/imm.12233

Ancsin, J. B. (2003). Amyloidogenesis: Historical and modern observations point to heparan sulfate proteoglycans as a major culprit. *Amyloid*, *10*(2), 67–79. https://doi.org/10.3109/13506120309041728

Blasco, H., Veyrat-Durebex, C., Bocca, C., Patin, F., Vourc'H, P., Kouassi Nzoughet, J., … Reynier, P. (2017). Lipidomics Reveals Cerebrospinal-Fluid Signatures of ALS. *Scientific Reports*. https://doi.org/10.1038/s41598-017-17389-9

Bradley, E. (2012). Incorporating biomarkers into clinical trial designs: points to consider. *Nat Biotechnol*, *30*(7), 596–599. https://doi.org/10.1038/nbt.2296

Cipolat Mis, M. S., Brajkovic, S., Frattini, E., Di Fonzo, A., & Corti, S. (2016). Autophagy in motor neuron disease: Key pathogenetic mechanisms and therapeutic targets. *Molecular and Cellular Neuroscience*, *72*, 84–90. https://doi.org/10.1016/J.MCN.2016.01.012

Conboy, I. M., Conboy, M. J., Wagers, A. J., Girma, E. R., Weismann, I. L., & Rando, T. A. (2005). Rejuvenation of aged progenitor cells by exposure to a young systemic environment. *Nature*. https://doi.org/10.1038/nature03260

Delaye, J. B., Patin, F., Piver, E., Bruno, C., Vasse, M., Vourc'h, P., … Blasco, H. (2017). Low IDL-B and high LDL-1 subfraction levels in serum of ALS patients. *Journal of the Neurological Sciences*. https://doi.org/10.1016/j.jns.2017.07.019

DeWitt, D. A., Richey, P. L., Praprotnik, D., Silver, J., & Perry, G. (1994). Chondroitin sulfate proteoglycans are a common component of neuronal inclusions and astrocytic reaction in neurodegenerative diseases. *Brain Research*, *656*(1), 205–209. https://doi.org/10.1016/0006-8993(94)91386-2

Finn, T. E., Nunez, A. C., Sunde, M., & Easterbrook-Smith, S. B. (2012). Serum albumin prevents protein aggregation and amyloid formation and retains chaperone-like activity in the presence of physiological ligands. *J Biol Chem*, *287*(25), 21530–21540. https://doi.org/10.1074/jbc.M112.372961

Forostyak, S., Homola, A., Turnovcova, K., Svitil, P., Jendelova, P., & Sykova, E. (2014). Intrathecal delivery of mesenchymal stromal cells protects the structure of altered perineuronal nets in SOD1 rats and amends the course of ALS. *Stem Cells*. https://doi.org/10.1002/stem.1812

Foyez, T., Takeda-Uchimura, Y., Ishigaki, S., Narentuya, N., Zhang, Z., Sobue, G., … Uchimura, K. (2015). Microglial keratan sulfate epitope elicits in central nervous tissues of transgenic model mice and patients with amyotrophic lateral sclerosis. *American Journal of Pathology*, *185*(11), 3053–3065. https://doi.org/10.1016/j.ajpath.2015.07.016

Friedrich, R. P., Tepper, K., Rönicke, R., Soom, M., Westermann, M., Reymann, K., … Fändrich, M. (2010). Mechanism of amyloid plaque formation suggests an intracellular basis of Abeta pathogenicity. *Proceedings of the National Academy of Sciences of the United States of America*, *107*(5), 1942–1947. https://doi.org/10.1073/pnas.0904532106

Garbuzova-Davis, S., Hernandez-Ontiveros, D. G., Rodrigues, M. C., Haller, E., Frisina-Deyo, A., Mirtyl, S., … Sanberg, P. R. (2012). Impaired blood-brain/spinal cord barrier in ALS patients. *Brain Res*, *1469*, 114–128. https://doi.org/10.1016/j.brainres.2012.05.056

Hirano, K., Ohgomori, T., Kobayashi, K., Tanaka, F., Matsumoto, T., Natori, T., … Kadomatsu, K. (2013). Ablation of Keratan Sulfate Accelerates Early Phase Pathogenesis of ALS. *PLoS ONE*. https://doi.org/10.1371/journal.pone.0066969

Holmes, B. B., DeVos, S. L., Kfoury, N., Li, M., Jacks, R., Yanamandra, K., … Diamond, M. I. (2013). Heparan sulfate proteoglycans mediate internalization and propagation of specific proteopathic seeds. *Proceedings of the National Academy of Sciences*. https://doi.org/10.1073/pnas.1301440110

Hoyles, L., Snelling, T., Umlai, U.-K., Nicholson, J. K., Carding, S. R., Glen, R. C., & McArthur, S. (2018). Microbiome–host systems interactions: protective effects of propionate upon the blood–brain barrier. *Microbiome 2018 6:1*, *6*(1), 55. https://doi.org/10.1186/s40168-018-0439-y

Lee, S., & Kim, H.-J. (2015). Prion-like Mechanism in Amyotrophic Lateral Sclerosis: are Protein Aggregates the Key? *Experimental Neurobiology*, *24*(1), 1–7. https://doi.org/10.5607/en.2015.24.1.1

Lehallier, B., Gate, D., Schaum, N., Nanasi, T., Lee, S. E., Yousef, H., … Wyss-Coray, T. (2019). Undulating changes in human plasma proteome profiles across the lifespan. *Nature Medicine*, *25*(12), 1843–1850. https://doi.org/10.1038/s41591-019-0673-2

Leoni, E., Bremang, M., Mitra, V., Zubiri, I., Jung, S., Lu, C.-H., … Malaspina, A. (2019). Combined Tissue-Fluid Proteomics to Unravel Phenotypic Variability in Amyotrophic Lateral Sclerosis. *Scientific Reports*, *9*(1). https://doi.org/10.1038/s41598-019-40632-4

Ling, S. C., Polymenidou, M., & Cleveland, D. W. (2013). Converging mechanisms in ALS and FTD: disrupted RNA and protein homeostasis. *Neuron*, *79*(3), 416–438. https://doi.org/10.1016/j.neuron.2013.07.033

Lu, C.-H., Petzold, A., Kalmar, B., Dick, J., Malaspina, A., & Greensmith, L. (2012). Plasma Neurofilament Heavy Chain Levels Correlate to Markers of Late Stage Disease Progression and Treatment Response in SOD1(G93A) Mice that Model ALS. *PLoS One*, *7*(7), e40998. https://doi.org/10.1371/journal.pone.0040998

Lu, C. H., Kalmar, B., Malaspina, A., Greensmith, L., & Petzold, A. (2011). A method to solubilise protein aggregates for immunoassay quantification which overcomes the neurofilament “hook” effect. *J*

Neurosci Methods, *195*(2), 143–150. https://doi.org/10.1016/j.jneumeth.2010.11.026

Lu, C. H., Macdonald-Wallis, C., Gray, E., Pearce, N., Petzold, A., Norgren, N., … Malaspina, A. (2015). Neurofilament light chain: A prognostic biomarker in amyotrophic lateral sclerosis. *Neurology*, *84*(22), 2247–2257. https://doi.org/10.1212/wnl.0000000000001642

Lu, C. H., Petzold, A., Topping, J., Allen, K., Macdonald-Wallis, C., Clarke, J., … Malaspina, A. (2015). Plasma neurofilament heavy chain levels and disease progression in amyotrophic lateral sclerosis: insights from a longitudinal study. *J Neurol Neurosurg Psychiatry*, *86*(5), 565–573. https://doi.org/10.1136/jnnp-2014-307672

Ludolph, A., Drory, V., Hardiman, O., Nakano, I., Ravits, J., Robberecht, W., & Shefner, J. (2015). A revision of the El Escorial criteria - 2015. *Amyotrophic Lateral Sclerosis & Frontotemporal Degeneration*, Vol. 16, pp. 291–292. https://doi.org/10.3109/21678421.2015.1049183

Lyon, M. S., Wosiski-Kuhn, M., Gillespie, R., Caress, J., & Milligan, C. (2019). Inflammation, Immunity, and amyotrophic lateral sclerosis: I. Etiology and pathology. *Muscle and Nerve*. https://doi.org/10.1002/mus.26289

McKinley, M. P., Bolton, D. C., & Prusiner, S. B. (1983). A protease-resistant protein is a structural component of the scrapie prion. *Cell*, *35*(1), 57–62.

Ngo, S. T., & Steyn, F. J. (2015). The interplay between metabolic homeostasis and neurodegeneration: insights into the neurometabolic nature of amyotrophic lateral sclerosis. *Cell Regen (Lond)*, *4*(1), 5. https://doi.org/10.1186/s13619-015-0019-6

Niccoli, T., Partridge, L., & Isaacs, A. M. (2017). Ageing as a risk factor for ALS/FTD. *Human Molecular Genetics*, *26*(R2), R105–R113. https://doi.org/10.1093/hmg/ddx247

Nishitsuji, K. (2018). Heparan sulfate S-domains and extracellular sulfatases (Sulfs): their possible roles in protein aggregation diseases. *Glycoconjugate Journal*, 387–396. https://doi.org/10.1007/s10719-018-9833-8

Palamiuc, L., Schlagowski, A., Ngo, S. T., Vernay, A., Dirrig-Grosch, S., Henriques, A., … Rene, F. (2015). A metabolic switch toward lipid use in glycolytic muscle is an early pathologic event in a mouse model of amyotrophic lateral sclerosis. *EMBO Mol Med*, *7*(5), 526–546. https://doi.org/10.15252/emmm.201404433

Perez-Riverol, Y., Csordas, A., Bai, J., Bernal-Llinares, M., Hewapathirana, S., Kundu, D. J., … Vizcaíno, J. A. (2019). The PRIDE database and related tools and resources in 2019: Improving support for quantification data. *Nucleic Acids Research*. https://doi.org/10.1093/nar/gky1106

Petzold, A., Tisdall, M. M., Girbes, A. R., Martinian, L., Thom, M., Kitchen, N., & Smith, M. (2011). In vivo monitoring of neuronal loss in traumatic brain injury: A microdialysis study. *Brain*.

https://doi.org/10.1093/brain/awq360

Polymenidou, M., & Cleveland, D. W. (2011). The seeds of neurodegeneration: prion-like spreading in ALS. *Cell*, *147*(3), 498–508. https://doi.org/10.1016/j.cell.2011.10.011

Quintana, C., Cowley, J. M., & Marhic, C. (2004). Electron nanodiffraction and high-resolution electron microscopy studies of the structure and composition of physiological and pathological ferritin. *Journal of Structural Biology*. https://doi.org/10.1016/j.jsb.2004.03.001

Russell, C. L., Mitra, V., Hansson, K., Blennow, K., Gobom, J., Zetterberg, H., … Pike, I. (2016). Comprehensive Quantitative Profiling of Tau and Phosphorylated Tau Peptides in Cerebrospinal Fluid by Mass Spectrometry Provides New Biomarker Candidates. *Journal of Alzheimer's Disease*, *55*(1), 303–313. https://doi.org/10.3233/JAD-160633

Saez, I., & Vilchez, D. (2014). The Mechanistic Links Between Proteasome Activity, Aging and Age-related Diseases. *Curr Genomics*, *15*(1), 38–51. https://doi.org/10.2174/138920291501140306113344

Safar, J. G., Wille, H., Geschwind, M. D., Deering, C., Latawiec, D., Serban, A., … Prusiner, S. B. (2006). Human prions and plasma lipoproteins. *Proceedings of the National Academy of Sciences*. https://doi.org/10.1073/pnas.0604021103

Sana, B., Poh, C. L., & Lim, S. (2012). A manganese-ferritin nanocomposite as an ultrasensitive T2contrast agent. *Chemical Communications*. https://doi.org/10.1039/c1cc15189d

Sarrazin, S., Lamanna, W. C., & Esko, J. D. (2011). Heparan sulfate proteoglycans. *Cold Spring Harbor Perspectives in Biology*, *3*(7), 1–33. https://doi.org/10.1101/cshperspect.a004952

Sasaki, S. (2011). Autophagy in spinal cord motor neurons in sporadic amyotrophic lateral sclerosis. *J Neuropathol Exp Neurol*, *70*. https://doi.org/10.1097/NEN.0b013e3182160690

Shi, Y., Lin, S., Staats, K. A., Li, Y., Chang, W. H., Hung, S. T., … Ichida, J. K. (2018). Haploinsufficiency leads to neurodegeneration in C9ORF72 ALS/FTD human induced motor neurons. *Nat Med*. https://doi.org/10.1038/nm.4490

Shijo, T., Warita, H., Suzuki, N., Kitajima, Y., Ikeda, K., Akiyama, T., … Aoki, M. (2018). Aberrant astrocytic expression of chondroitin sulfate proteoglycan receptors in a rat model of amyotrophic lateral sclerosis. *Journal of Neuroscience Research*, *96*(2), 222–233. https://doi.org/10.1002/jnr.24127

Song, C., Guo, J., Liu, Y., & Tang, B. (2012). Autophagy and Its Comprehensive Impact on ALS. *International Journal of Neuroscience*, *122*(12), 695–703. https://doi.org/10.3109/00207454.2012.714430

Sullivan, P. M., Zhou, X., Robins, A. M., Paushter, D. H., Kim, D., Smolka, M. B., & Hu, F. (2016). The ALS/FTLD associated protein C9orf72 associates with SMCR8 and WDR41 to regulate the autophagy-

lysosome pathway. *Acta Neuropathologica Communications*. https://doi.org/10.1186/s40478-016-0324-5

Supattapone, S. (2012). Phosphatidylethanolamine as a prion cofactor: Potential implications for disease pathogenesis. *Prion*. https://doi.org/10.4161/pri.21826

Szelechowski, M., Amoedo, N., Obre, E., Léger, C., Allard, L., Bonneu, M., … Rossignol, R. (2018). Metabolic Reprogramming in Amyotrophic Lateral Sclerosis. *Scientific Reports*. https://doi.org/10.1038/s41598-018-22318-5

Tefera, T. W., & Borges, K. (2017). Metabolic dysfunctions in amyotrophic lateral sclerosis pathogenesis and potential metabolic treatments. *Frontiers in Neuroscience*. https://doi.org/10.3389/fnins.2016.00611

Terry, C., Wenborn, A., Gros, N., Sells, J., Joiner, S., Hosszu, L. L. P., … Wadsworth, J. D. F. (2016). Ex vivo mammalian prions are formed of paired double helical prion protein fibrils. *Open Biology*. https://doi.org/10.1098/rsob.160035

Villeda, S. A., Luo, J., Mosher, K. I., Zou, B., Britschgi, M., Bieri, G., … Wyss-Coray, T. (2011). The ageing systemic milieu negatively regulates neurogenesis and cognitive function. *Nature*. https://doi.org/10.1038/nature10357

Weids, A. J., Ibstedt, S., Tamas, M. J., & Grant, C. M. (2016). Distinct stress conditions result in aggregation of proteins with similar properties. *Sci Rep*, *6*, 24554. https://doi.org/10.1038/srep24554

Weksler, B. B., Subileau, E. A., Perrière, N., Charneau, P., Holloway, K., Leveque, M., … Couraud, P. O. (2005). Blood-brain barrier-specific properties of a human adult brain endothelial cell line. *FASEB Journal : Official Publication of the Federation of American Societies for Experimental Biology*, *19*(13), 1872–1874. https://doi.org/10.1096/fj.04-3458fje

Williams, S. A., Kivimaki, M., Langenberg, C., Hingorani, A. D., Casas, J. P., Bouchard, C., … Wareham, N. J. (2019). Plasma protein patterns as comprehensive indicators of health. *Nature Medicine*, *25*(12), 1851–1857. https://doi.org/10.1038/s41591-019-0665-2

Xia, K., Trasatti, H., Wymer, J. P., & Colon, W. (2016). Increased levels of hyper-stable protein aggregates in plasma of older adults. *Age (Dordr)*, *38*(3), 56. https://doi.org/10.1007/s11357-016-9919-9

Yang, H., & Hu, H. Y. (2016). Sequestration of cellular interacting partners by protein aggregates: implication in a loss-of-function pathology. *FEBS J*, *283*(20), 3705–3717. https://doi.org/10.1111/febs.13722

Zhang, B., Kirov, S., & Snoddy, J. (2005). WebGestalt: An integrated system for exploring gene sets in various biological contexts. *Nucleic Acids Research*, *33*(SUPPL. 2), 741–748. https://doi.org/10.1093/nar/gki475

Zhou, Z., Fan, J.-B., Zhu, H.-L., Shewmaker, F., Yan, X., Chen, X., … Liang, Y. (2009). Crowded Cell-like Environment Accelerates the Nucleation Step of Amyloidogenic Protein Misfolding. *Journal of Biological Chemistry*, *284*(44), 30148–30158. https://doi.org/10.1074/jbc.M109.002832

Zubiri, I., Lombardi, V., Bremang, M., Mitra, V., Nardo, G., Adiutori, R., … Malaspina, A. (2018). Tissue-enhanced plasma proteomic analysis for disease stratification in amyotrophic lateral sclerosis. *Molecular Neurodegeneration*, *13*(1), 60. https://doi.org/10.1186/s13024-018-0292-2

Figures

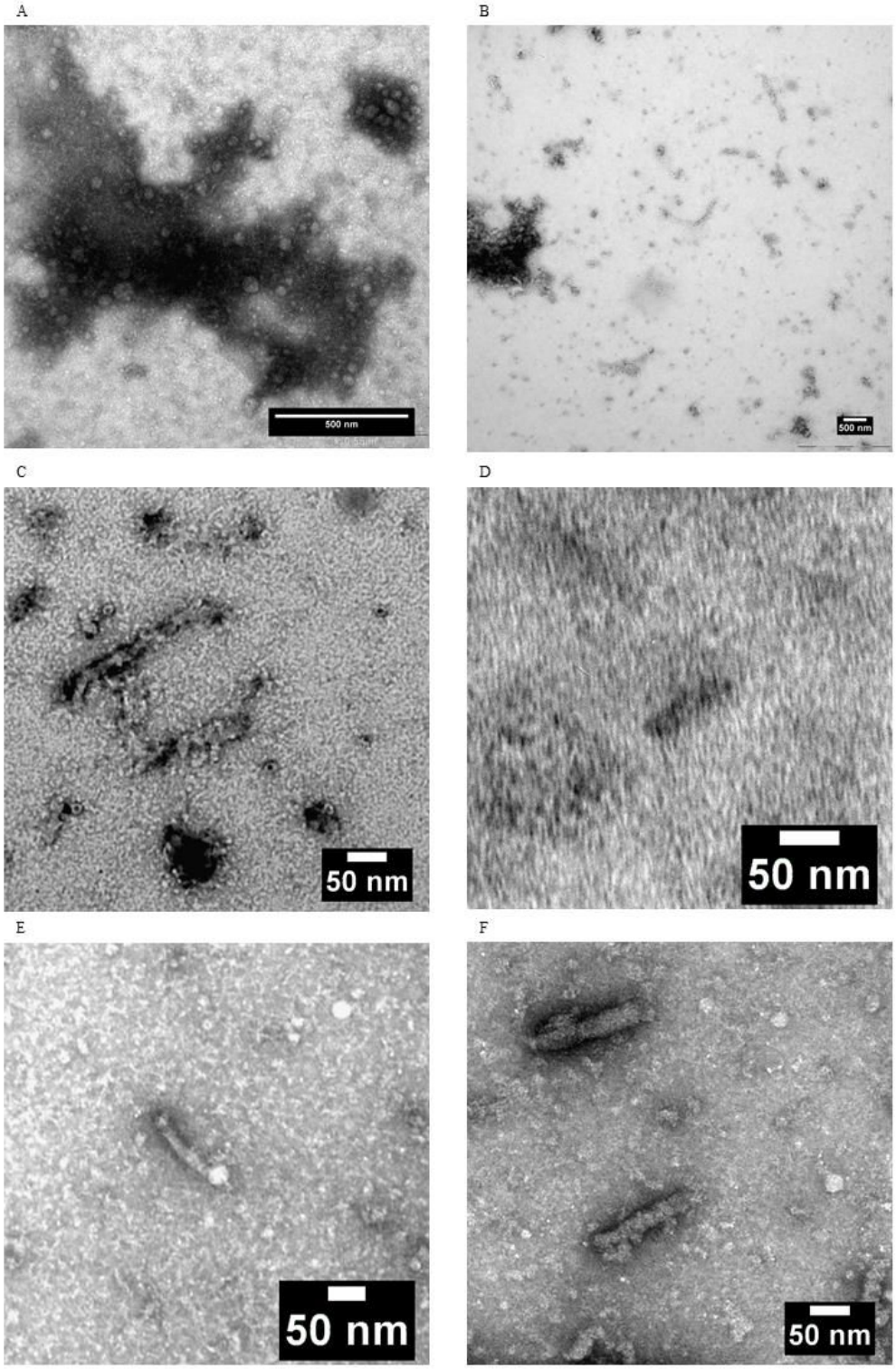

Figure 1

Micrographs of circulating protein aggregates (CPA) and brain protein aggregates (BPA) taken by transmission electron microscopy. (A) grid micrograph after CPA sample loading showing an amorphous globular formation with adjacent and/or superimposed smaller rounded particles (which may be formed of lipoproteins). (B) grid micrograph of BPA showing amorphous electron-dense (left-hand side) as well as short filamentous and small round formations. (C) Details of filamentous and of donut-like particles

detected in BPA micrographs. (D, E, F) Micrograph grids of CPA showing 13 to 20 nm thick and 70 to 145 nm long fragments. Scale bar on the lower right-hand corner of each micrograph.

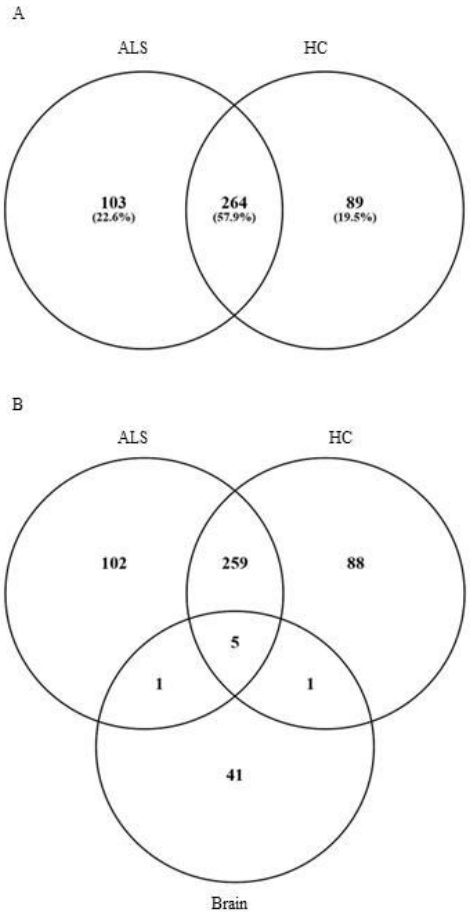

Figure 2

Comparison of circulating protein aggregates (ALS and HC) and brain protein aggregates (ALS) composition. (A) Venn diagram showing CPA proteins unique to or shared by ALS and HC. (B) Venn diagram showing HC and ALS CPA proteins shared by brain aggregates. Five proteins were expressed in

all 3 aggregate groups (actin cytoplasmic 1, tubulin alpha-4A chain isoform 2, clathrin heavy chain 1 isoform 2, collagen alpha-1(VI) and plectin isoform 7), while brain aggregates shared only one protein with ALS and HC CPA (cytoplasmic dynein 1 heavy chain 1 and collagen alpha-2(VI), respectively).

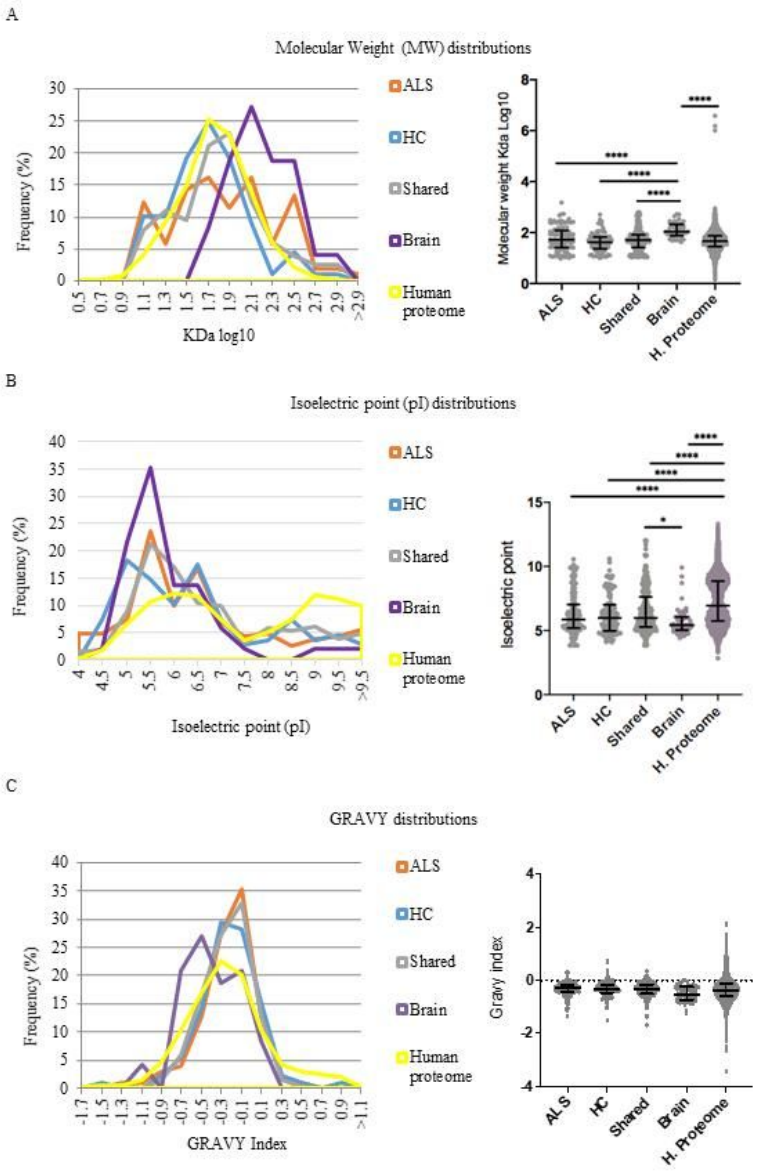

Figure 3

Aggregation propensity of proteins in blood and brain aggregates from ALS and HC compared to the Human proteome. Molecular weight (MW) (A), isoelectric point (pI) (B) and hydrophobicity (GRAVY index)

(C), known to affect aggregation propensity, are compared across proteins found to be expressed only in ALS and HC CPA (ALS and HC respectively), proteins shared between ALS and HC CPA datasets (Shared), proteins within brain aggregates (Brain) and in the entire human proteome. The distribution plots show the dispersion of the samples with relative frequency, while the violin plots show median and interquartile ranges. Statistical analysis was performed using one-way ANOVA, Kruskal-Wallis test with Dunn's multiple comparison as post-test for group analysis with * expressing the level of significance (*: p = 0.0251; ****: p < 0.0001).

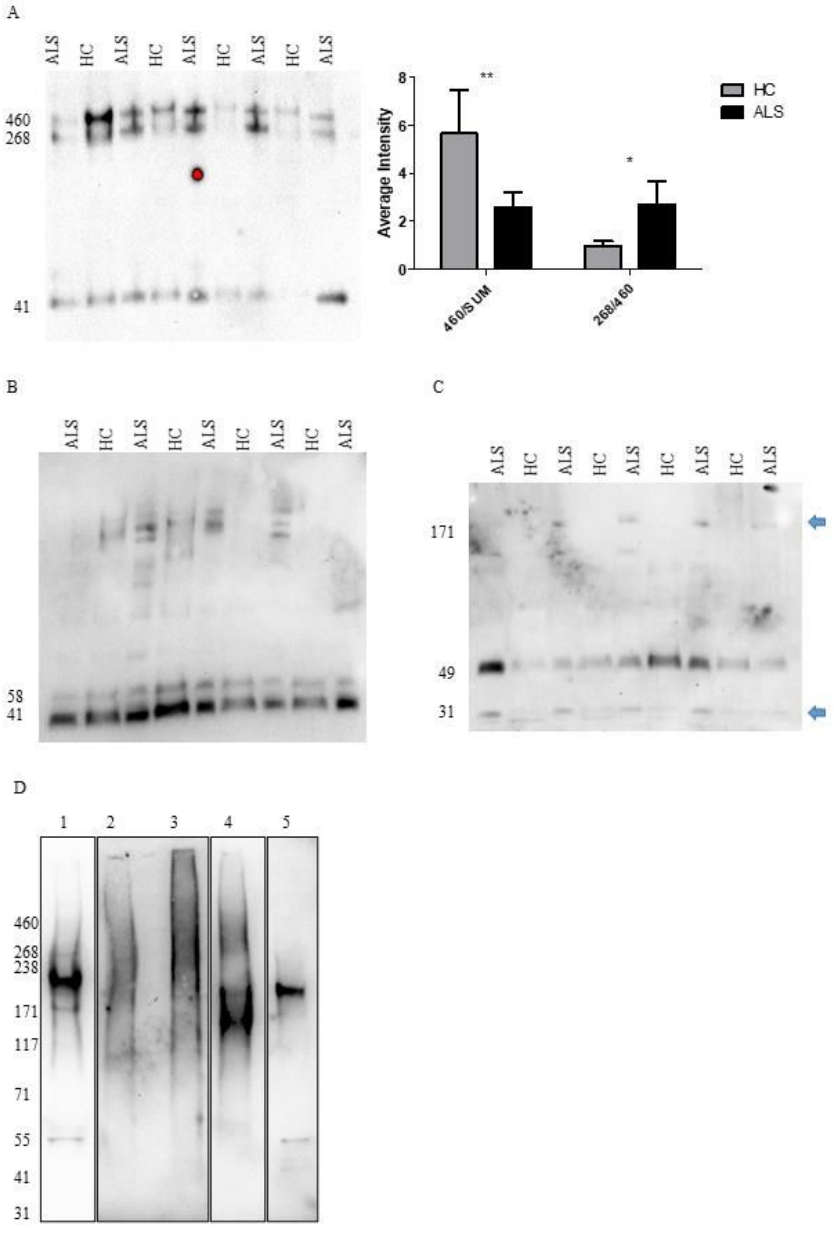

Figure 4

Western blot analysis of neurofilament heavy chain within circulating protein aggregates after proteases digestion. Undigested CPA (A) show NfH bands at 460, 268 and 41 KDa (268 KDa is NfH expected molecular weight). The ratio between the 460 KDa band and the the sum of all NfH band intensities (SUM, 460/SUM) is higher in HC (p= 0.032), while the ratio between the 268 and 460 bands (268/460) is higher in ALS (p= 0.018). Calpain digestion (B) shows 58 and 41 KDa bands in all samples with no difference in expression. The enterokinase digestion profile of NfH (C) shows a 49 KDa band uniformly expressed across samples and additional 171 and 31 KDa bands only in ALS patients (blue arrows). Undigested NfH in ALS brain protein aggregates (BPA; D, lane 1) and after digestion with chymotrypsin (lane 2), enterokinase (lane 3), calpain (lane 4) and brain lysate lane 5. To maximise band visualization, time exposure was for lane 1 at 10.1 seconds, lane 4 and 5 at 58.4 seconds and lane 2 and 3 at 278.8 seconds. In D, the lanes have been rearranged to simplify comparison with CPA data shown in A, B and C. The original blot is included in the Supplementary Material.

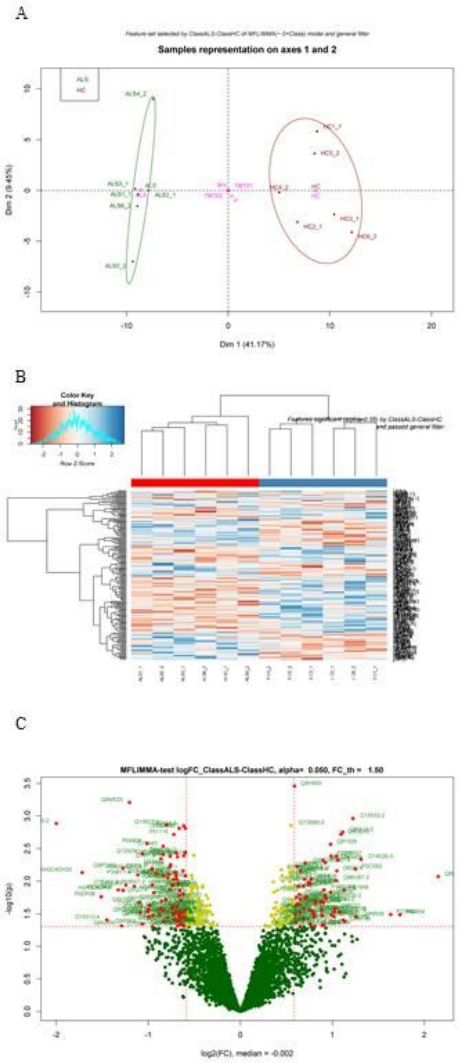

Figure 5

TMTcalibrator™ proteomic analysis. (A) Principal component analysis (PCA) showing a separation between the ALS and HC experimental groups regulated features at protein level. Dimension 1 or the variance between the two experimental groups (ALS and HC) is 41.17% of the entire variance; dimension 2 or variance between 10plexes (TMT01 and TMT02) is 9.45% of the entire variance. (B) Heatmap showing the distribution of the regulated features and their clustering. The regulated features are

distributed vertically, reported as Uniprot IDs on the right-hand side and relative clustering on the left-hand side. Analytical samples are distributed horizontally, with sample names at the bottom and relative clustering at the top of the heatmaps. The color key histogram at the top left side shows the distribution of the features and the heatmap color coding. (C) The volcano plot shows the distribution of the proteins identified by TMT proteomic study according to their fold change (FC) expressed as log2 (fold change ALS/HC) (logFC) in the x axis and according to p-value expressed as –log10 (p-value) in the y axis. Protein groups were considered regulated if p-value < 0.05 and logFC < -0.58 or > 0.58. Red dots are regulated features, yellow dots are features with a significant p-value (p < 0.05) and logFC between -0.58 and 0.58 while green dots are not regulated protein groups (p > 0,05). Uniprot IDs are reported beside the dots with significant p-value.

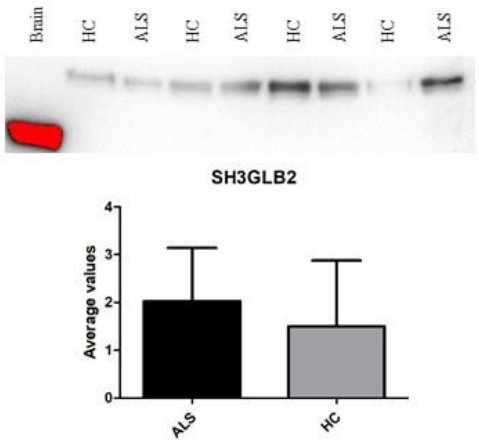

Figure 6

Western blot analysis of Endophilin-B2 (SH3GLB2) in plasma CPA from ALS patients and healthy controls. Samples were normalized to HC6 density and the average values with relative standard deviation for the ALS (n=4) and Control (n=4) groups were plotted onto the chart. A brain lysate sample is also included (1st lane, red band, indicating signal saturation) which showed an endophilin-B2 band at a lower molecular weight than the bands detected in CPA. Immunodetection confirmed the SH3GLB2 higher

level of expression in the ALS CPA compared to control (logFC= 0.34), but without being statistically significant (p= 0.57).

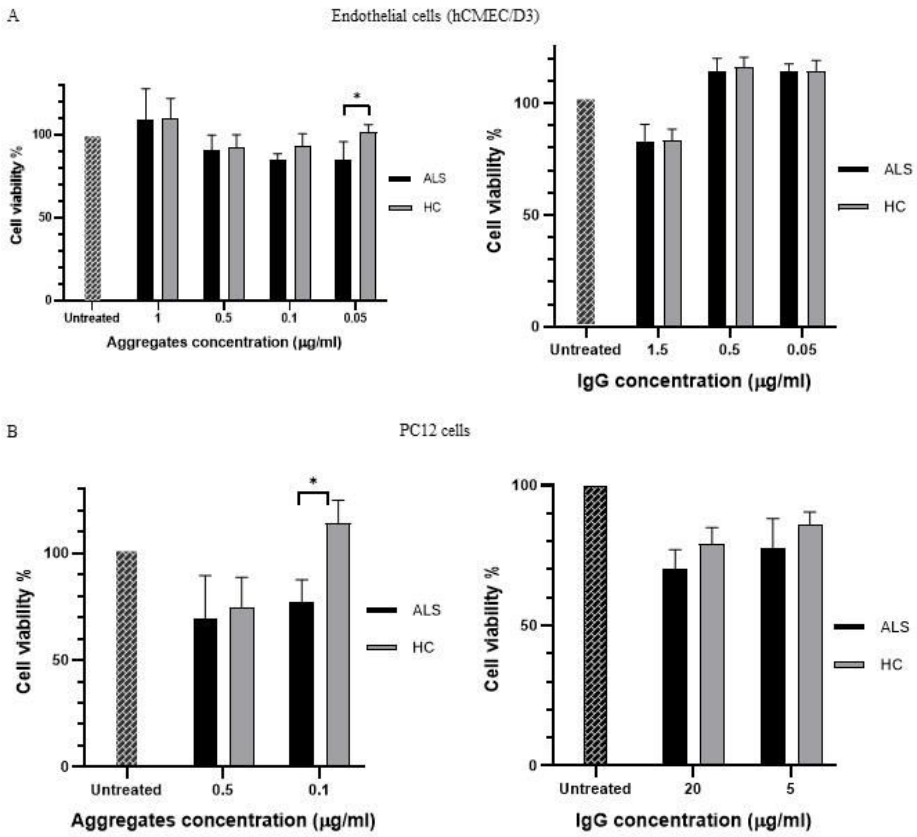

Figure 7

Cell viability after treatment with aggregates, solubilized aggregates and immunoglobulins extracted from plasma samples. The figure shows the percentage of endothelial (hCMEC/D3) and PC12 living cells (A and B) after treatment with different concentrations of CPA and IgG from ALS and HC. Cells treated

with ALS CPA showed a statistically significant lower cell viability compared to HC CPA treated cells at 0,05 µg/ml (p= 0.031; endothelial cells, A) and at 0,1 µg/ml (p= 0.029; PC12 cells, B). IgG had minor effect on all cell type viability with no difference between ALS and HC. CPA proteins were solubilized with 8M urea before PC12 cells treatment. Significance was tested by two-way ANOVA and Tukey HSD test.

Supplementary Files

This is a list of supplementary files associated with this preprint. Click to download.

- supplementaryinformation.docx